INTERNATIONAL JOURNAL OF CLIMATOLOGY
Int. J. Climatol. **33**: 265–276 (2013)
Published online 3 January 2012 in Wiley Online Library
(wileyonlinelibrary.com) DOI: 10.1002/joc.3419

The impacts of the summer Asian Jet Stream biases on surface air temperature in mid-eastern China in IPCC AR4 models

Xin Wang,[a] Wen Zhou,[a]* Dongxiao Wang[b] and Chunzai Wang[c]

[a] *Guy Carpenter Asia-Pacific Climate Impact Centre, School of Energy and Environment, City University of Hong Kong, Hong Kong, China*
[b] *State Key Laboratory of Tropical Oceanography, South China Sea Institute of Oceanology, Chinese Academy of Sciences, Guangzhou, China*
[c] *NOAA/Atlantic Oceanographic and Meteorological Laboratory, Miami, FL, USA*

ABSTRACT: One of the great model biases in simulating the East Asian summer monsoon are the warming bias of the summer surface air temperature (SAT) in mid-eastern China in the late 1970s. Previous studies have found that the summer equatorward displacement of the Asian Jet Stream (AJS) could result in SAT cooling in mid-eastern China in the past half century. This paper focuses on the relationship of the meridional displacement bias of the Asian Jet Stream (AJS) with the SAT bias in mid-eastern China in 22 IPCC AR4 models. On the basis of 20C3M simulation outputs, the bias analyses show that the summer SAT bias in mid-eastern China are closely linked to the bias of the subtropical upper-level zonal wind around the AJS core.

Climatologically, the summer AJS cores in more than half of IPCC models are north of the observed one, and most of models underestimate the intensity of the AJS. Ten models (bccr_bcm2_0, cccma_cgcm3_1_t63, cnrm_cm3, gfdl_cm_2_0, gfdl_cm2_1, ipsl_cm4, miroc3_2_hires, mpi_echam5, ncar_ccsm3_0, and ukmo_hadgem1) are able to capture the AJS meridional displacement – the distinct feature of the summer AJS – for the influences of climate in eastern China. Among these ten models, bccr_bcm2_0, cccma_cgcm3_1_t63, miroc3_2_hires, mpi_echam5 and ncar_ccsm3_0 fail to simulate the multi-decadal variations of the AJS and cccma_cgcm3_1_t63, cnrm_cm3, ipsl_cm4, mpi_echam5, and ukmo_hadgem1 underestimate large-scale circulations associated with the AJS over eastern China. Thus, merely two models, gfdl_cm_2_0 and gfdl_cm2_1, have the ability in successfully simulating the SAT cooling in mid-eastern China during the late 1970s. These results imply that a good simulation of the AJS is important for weather and climate forecasts and assessments in eastern China. Copyright © 2012 Royal Meteorological Society

KEY WORDS jet stream; surface air temperature; IPCC AR4

Received 18 January 2011; Revised 15 September 2011; Accepted 23 November 2011

1. Introduction

In the past half century, the most remarkable feature associated with climate changes over China is a moderate summer (June–July–August, JJA) surface cooling trend over mid-eastern China (Zhou and Yu, 2006; Yu *et al.*, 2010), which is in contrast to the common warming trend elsewhere (Jones *et al.*, 1999; Folland *et al.*, 2001a, 2001b). The natural and anthropogenic forcing are possible reasons of summer surface cooling variation in mid-eastern China in the late 1970s (Qian and Giorgi, 1999; Xu, 2001; Menon *et al.*, 2002; Qian *et al.*, 2003; Ueda *et al.*, 2006; Li *et al.*, 2007). Some studies emphasized that this summer cooling may be attributed to the multi-decadal variation of the large-scale summer monsoon circulations over eastern China (Yu *et al.*, 2004; Zhou *et al.*, 2006; Ding *et al.*, 2009). Since the late 1970s, the East Asian summer monsoon (EASM) has experienced a distinct multi-decadal variability with a weakening monsoon circulation of flood (drought) in southern (northern) China (Ding and Sun, 2003; Yu *et al.*, 2004; Yu and Zhou, 2007; Ding *et al.*, 2008). The recent warming in the tropical Pacific and Indian Oceans (Nitta and Hu, 1996; Gong and Ho, 2003; Hu *et al.*, 2003) could also cause excessive rainfall, and thus induce surface temperature cooling in mid-eastern China. In addition to the surface cooling, a distinctive strong tropospheric cooling is also found in East Asia during late summer. Yu *et al.* (2004) suggested that the stratospheric temperature changes might be responsible for a strong tropospheric cooling over East Asia.

Numerical models have successfully simulated some large-scale aspects of climate changes observed during the instrumental period (Raisanen, 2007), but the ability of models simulating the EASM is not yet satisfactory (Liang *et al.*, 2001; Zhou and Yu, 2006; Sun and Ding, 2008). Few IPCC AR4 climate models could reproduce the surface cooling change in mid-eastern China in the late 1970s even if time-varying forcing of

* Correspondence to: W. Zhou, Guy Carpenter Asia-Pacific Climate Impact Centre, School of Energy and Environment, City University of Hong Kong, Hong Kong, China. E-mail: wenzhou@cityu.edu.hk

anthropogenic aerosols including black carbon were prescribed (Zhou and Yu, 2006). Ensemble simulations of Asian–Australian summer rainfall anomalies for an El Niño event in 11 atmospheric GCMs were considerably poor (Wang *et al*., 2004). Through analysing AMIP GCM biases in eastern China, Liang *et al*. (2001) found the simulated summer monsoon over eastern China is prolonged but weak. Although IPCC AR4 climate models can simulate mean summer monsoon precipitation over eastern China, their performances on simulating multi-decadal changes in summer precipitation over eastern China are rather poor (Sun and Ding, 2008). The reasons of these models biases are complicated and may be caused by the internal processes, external forcing, and model parameterisations, and so on. All IPCC AR4 models include the increase of anthropogenic greenhouse gases and anthropogenic aerosols in 20th century simulation, but the details of the forcing vary with models (Zhou and Yu, 2006). Different natural forcing agents are involved in individual models, and thus, make direct inter-comparisons of simulations difficult.

The summer monsoon over eastern China is highly energetic and has been teleconnected. Thus, simulation biases are systematic (Liang *et al*., 2001; Sun and Ding, 2008). Liang and Wang (1998) indicated that the north-south displacement of the tropospheric westerly jet plays an important role in determining the monsoon onset and retreat. Both the observed (Lau *et al*., 2000; Liao *et al*., 2004) and modelling results (Liang *et al*., 2001; Zhang and Guo, 2005) have shown that an equatorward Asian Jet Stream (AJS) displacement in boreal summer causes more rainfall and cool surface air temperature (SAT) over south-central China via the associated anomalous meridional circulations (Liang *et al*., 2001; Zhang and Guo, 2005; Yu and Zhou, 2007). Yu *et al*. (2004) also found that the shifting southward upper-level westerly jet stream over East Asia may result in tendency surface-cooling in the downstream of the Tibetan Plateau. On the basis of the dynamical connections between the summer AJS and surface climate in eastern China, the purpose of this study is to investigate the performances of the AJS variations and the relationships between AJS and the mid-eastern China summer SAT in IPCC AR4 models.

The paper is organized as follows. The details of observed datasets and model outputs are presented in Section 2. Section 3 shows the relationships between SAT and AJS biases. To illustrate the influences of AJS biases on SAT in mid-eastern China, the performances of models on AJS are firstly assessed in detail in Section 4. Then, the performances of dominant physical processes connecting the AJS with the summer SAT in mid-eastern China are described in Section 5. Discussion and summary are given in Section 6.

2. Data and methothdology

2.1. Datasets

The monthly National Centers for Environmental Prediction/National Center for Atmospheric Research (NCEP/NCAR) reanalysis dataset (Kistler *et al*., 2001) and 22 IPCC AR4 models (20C3M experiments) outputs in summer during 1961–1999 are used. The IPCC AR4 models are shown in Table I. For the convenience of comparison, model outputs were linearly interpolated to the

Table I. Model names and resolutions.

No.	Model experiment acronym	IPCC ID	Model approximate resolution
1	bcc_cm1	BCC-CM1	1.9 × 1.9
2	bccr_bcm2_0	BCCR-BCM2.0	2.8 × 2.8
3	cccma_cgcm3_1	CGCM3.1	3.7 × 3.7
4	cccma_cgcm3_1_t63		2.8 × 2.8
5	cnrm_cm3	CNRM-CM3	2.8 × 2.8
6	csiro_mk3_0	CSIRO-MK3.0	1.9 × 1.9
7	gfdl_cm2_0	GFDL-CM2.0	2.5 × 2.0
8	gfdl_cm2_1	GFDL-CM2.1	2.5 × 2.0
9	giss_aom	GISS-AOM	4.0 × 3.0
10	giss_model_e_h	GISS-EH	5.0 × 4.0
11	giss_model_e_r	GISS-ER	5.0 × 4.0
12	iap_fgoals1_0_g	FGOALS-g1.0	2.8 × 3.0
13	inmcm3_0	INM-CM3.0	5.0 × 4.0
14	ipsl_cm4	IPSL-CM4	3.7 × 2.5
15	miroc3_2_hires	MIROC3.2 (hires)	1.1 × 1.1
16	miroc3_2_medres	MIROC3.2 (medres)	2.8 × 2.8
17	mpi_echam5	ECHAM5=MPI-OM	1.9 × 1.9
18	mri_cgcm2_3_2a	MRI-CGCM2.3.2	2.8 × 2.8
19	ncar_ccsm3_0	CCSM3	1.4 × 1.4
20	ncar_pcm1	PCM	2.8 × 2.8
21	ukmo_hadcm3	UKMO-HadCM3	3.7 × 2.5
22	ukmo_hadgem1	UKMO-HadGEM1	1.9 × 1.2

same 2.5° × 2.5° latitude–longitude grid as from the NCEP/NCAR reanalysis. The 156 stations' monthly SAT in Mainland China during 1961–1999 compiled by the Chinese Meteorological Administration are also used in this study.

2.2. Uncentred correlation

To illustrate the relationship of two variables' biases in coupled models, we compute the uncentred correlation coefficients. The uncentred correlation is different from the conventional correlation in that it uses zero as reference rather than the mean value. The uncentred correlation is calculated by the following:

$$r = \frac{1}{n}\sum_{i=1}^{n}\left(\frac{x_i}{\sqrt{\frac{1}{n}\sum_{i=1}^{n}{x_i}^2}}\right)\left(\frac{y_i}{\sqrt{\frac{1}{n}\sum_{i=1}^{n}{y_i}^2}}\right) = \frac{\sum_{i=1}^{n}x_i y_i}{\sqrt{\sum_{i=1}^{n}{x_i}^2}\sqrt{\sum_{i=1}^{n}{y_i}^2}} \qquad 1$$

where x and y are the two variables with size of n.

From the mathematical viewpoint, the uncentred correlation coefficient is the scalar product of the unit vectors in the directions of X and Y and, thus, is equal to the cosine of the angle between the two data vectors in an n-dimensional space. Since the vector X or Y describes the bias, a value of r close to 1 indicates that the two biases have similar directions, i.e. very similar profiles; a value of r close to 0 indicates little similarity, and close to −1 indicates that the two behave oppositely.

3. Relationship between AJS and SAT biases in mid-eastern China

Compared to the global surface warming during 1978–1997 (Jones *et al.*, 1999), the SAT cooling in mid-eastern China during boreal summer is distinct (Zhou and Yu, 2006). Observation shows that the summer SAT cooling in mid-eastern China is about 0.8 °C. As shown in Figure 1, most CGCMs participating IPCC AR4 fail to capture this unique change, and almost all of them simulate the SAT warming during the second half of the 20th century. Only few models, such as gfdl2.0, gfdl2.1, and miroc3_2_medres, can simulate the observed boreal summer SAT cooling. However, their simulated cooling magnitudes are much smaller than the observations.

The climate over East Asia on interannual and longer timescales is strongly influenced by the subtropical upper-level zonal wind anomalies, particularly the changes of the AJS (Liang and Wang, 1998; Lau *et al.*, 2000; Liang

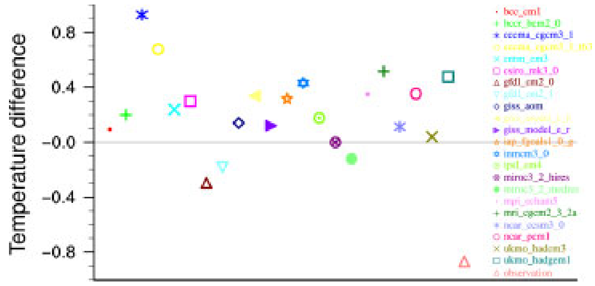

Figure 1. Differences of mean JJA SAT in mid-eastern China (25°–35°N, 105°–120 °E) between 1980 and 1999, and 1961 and 1976, from the IPCC-AR4 20C3M simulations and station observations. This figure is available in colour online at wileyonlinelibrary.com/journal/joc

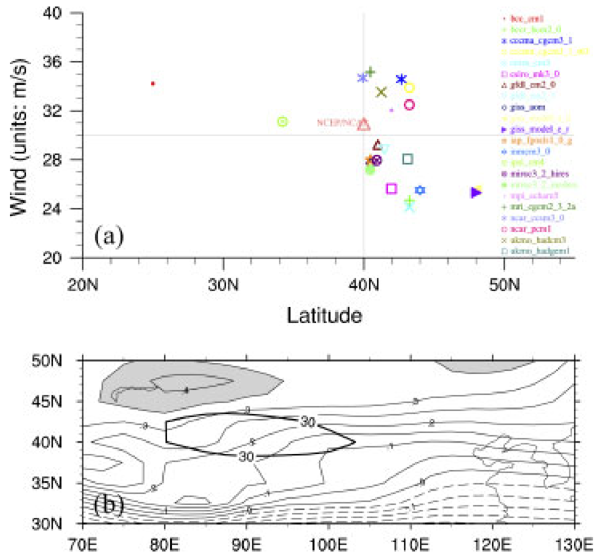

Figure 2. (a) The maximum of summer climatology zonal-averaged (75°–105 °E) zonal wind at 200 hPa and its location. (b) Uncentred correlation pattern between summer 200 hPa zonal wind biases and surface temperature biases averaged at (25°–35°N, 105°–120 °E). The shading is exceeding 90% significant level. The thick contour line is the 30 m/s zonal wind climatology at 200 hPa in JJA from 1961 to 1999 in NCEP/NCAR reanalysis. This figure is available in colour online at wileyonlinelibrary.com/journal/joc

et al., 2001; Liao *et al.*, 2004; Lu, 2004; Wang *et al.*, 2011). Climatologically, the core of the 200-hPa JJA AJS is located approximately at 40°N (Figure 2(a)). However, the maximum of simulated upper-level zonal wind averaged between 75° and 105 °E in most models are north to 40°N, and the differences of zonal wind magnitude between observation and simulations are also large. We hypothesize that the biases of the AJS location simulation could cause poor simulations of the SAT in mid-eastern China. In order to test this hypothesis, we investigate the systematic relationships between the upper-level zonal wind biases and summer SAT biases in mid-eastern China. The uncentred correlations between the biases of JJA zonal wind at 200 hPa and mid-eastern China SAT are used here. Using the NCEP/NCAR reanalysis dataset and station SAT dataset, the biases of 200-hPa JJA zonal wind in each grid point and area-averaged JJA SAT in mid-eastern China (25°–35 °N, 105°–120 °E) are firstly calculated for individual models. Then, the biases of zonal wind and surface temperature of each model are arranged sequentially, and their lengths are 22 × 39 (22 IPCC AR4 models over a 39-year period from 1961 to 1999. Note that the order sequence is not important). Finally, the uncentred correlations are calculated between these biases fields. Figure 2(b) shows the spatial pattern of correlation between upper-level zonal wind bias and mid-eastern China summer SAT bias. The significant positive correlation coefficients between upper-level zonal wind and mid-eastern China summer SAT biases are found to the north of the climatological location of the observed AJS (Figure 2(b)). The significant positive relationship suggests that the biases of summer SAT in mid-eastern China are not isolated, and are systematically linked to the biases of subtropical upper-level zonal wind.

4. Model performances of subtropical upper-level zonal wind

In order to clearly explain the linkage between the subtropical upper-level zonal wind biases and mid-eastern China SAT biases in CGCMs, the assessments on the ability of simulating summer zonal wind at 200 hPa are illustrated in this section. A primary prerequisite to judge a model performance is its ability to capture the multi-year average fields. As for climatology pattern of summer zonal wind at 200 hPa simulated by different models, the bcc_cm1 model fails to reproduce the summer climatology upper-level zonal wind in the subtropics (Figure 3(a)). Some models such as cccma_cgcm3_1, cccma_cgcm3_1_t63, mpi_echam5, mri_cgcm2_3_2a, ncar_ccsm3_0, ncar_pcm1, and ukmo_hadcm3, simulate stronger upper-level zonal wind than observations, while the simulations by the

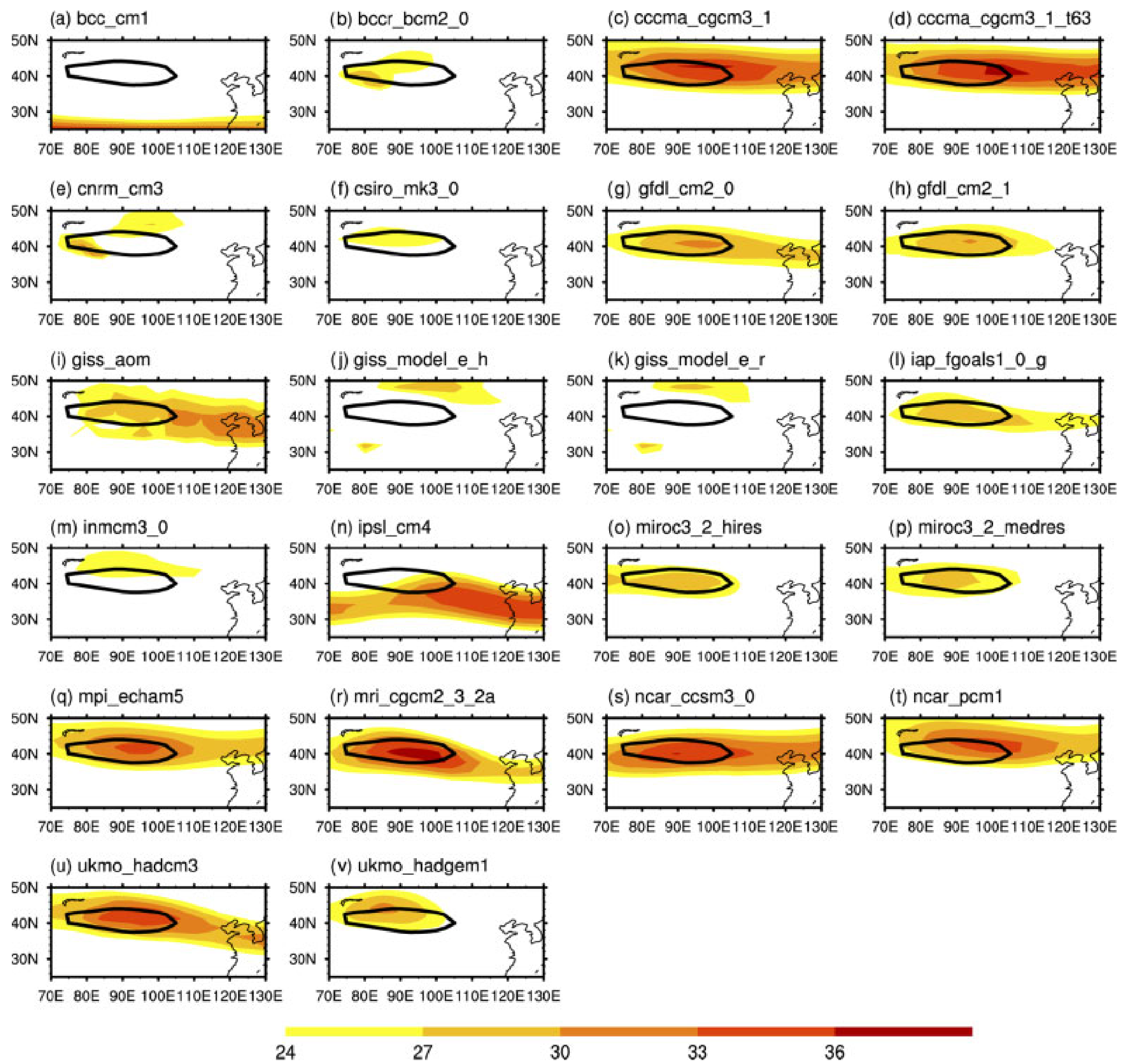

Figure 3. The bold lines represent the contours of 30 m/s zonal wind at 200 hPa in JJA from 1961 to 1999 in NCEP/NCAR reanalysis, and the shadings are the zonal wind at 200 hPa for IPCC models. This figure is available in colour online at wileyonlinelibrary.com/journal/joc

other models (i.e. bcc_cm1, bccr_bcm2_0, cnrm_cm3, csiro_mk3_0, gfdl_cm2_0, gfdl_cm2_1, giss_aom, giss_model_e_h, giss_model_e_r, iap_fgoals1_0_g, inmcm3_0, ipsl_cm4, miroc3_2_hires, miroc3_2_medres, and ukmo_hadgem1) underestimated zonal wind intensity. Also, it is found that the climatology of strong simulated zonal wind with more than 27 m/s (in most IPCC AR4 models) is located to the north of the observed AJS, and the bcc_cm1 and ipsl_cm4 model simulations are apparent to the south of the observed AJS (Figure 3(a) and (n)). Since the core of the summer AJS resides near 40°N along 75° – 105 °E (Figure 3), the comparisons of the maximum of climatology 200 hPa zonal wind averaged between 75° and 105 °E in Figure 2(a) show, apparently, the biases of the AJS. Figure 2(a) shows that only the simulation of ncar_ccsm3_0 is quite similar to the observation. The simulated AJS cores of the maximum of zonal-averaged zonal wind in 19 out of 22 models (bccr_bcm2_0, cccma_cgcm3_1, cccma_cgcm3_1_t63, cnrm_cm3, csiro_mk3_0, gfdl_cm2_0, gfdl_cm2_1, giss_aom, giss_model_e_h, giss_model_e_r, iap_fgoals1_0_g, inmcm3_0, miroc3_2_hires, miroc3_2_medres, mpi_echam5, mri_cgcm2_3_2a, ncar_pcm1, ukmo_hadcm3, and ukmo_hadgem1), are north of 40°N, while the simulated AJS cores by bcc_cm1 and ipsl_cm4 are at about 25°N and 34°N south of the observed location. In summary, the simulated climatology locations of the summer AJS in IPCC AR4 models are mostly north of the observed location.

We perform the empirical orthogonal function (EOF) analysis on the simulated summer zonal wind at 200 hPa in individual models and the NCEP/NCAR reanalysis (Figure 4). The observed first leading mode (Figure 4(w)) of upper-level zonal wind explaining 37.3% variance exhibits a meridional dipole structure with the zero line located around 40°N where the observed AJS core is located (Figure 3(w)), consistent to the previous results

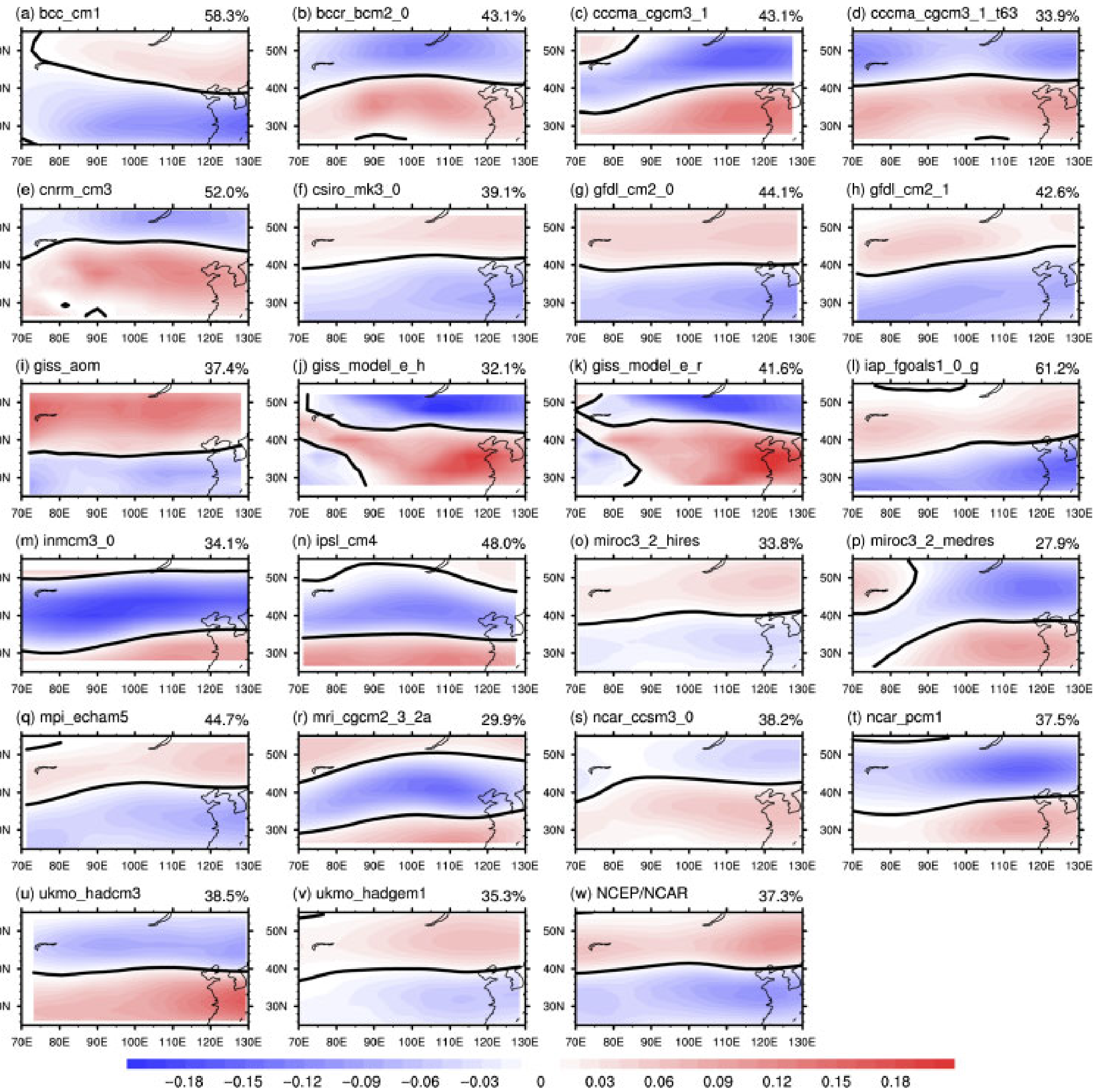

Figure 4. The patterns of the first leading EOF mode of the JJA zonal wind at 200 hPa for IPCC models and the NCAR/NCEP reanalysis. The bold lines represent the contours of zero. This figure is available in colour online at wileyonlinelibrary.com/journal/joc

(Gong and Ho, 2003; Lin and Lu, 2005; Zhang *et al*., 2008). This pattern indicates a strong meridionally oriented trough-ridge system influencing the climate over central and east Asia. Compared to the results of observation, most models are able to reproduce meridional dipole structure at about 40°N except for inmcm3_0 and mri_cgcm2_3_2a (Figure 4). However, compared with the first leading mode and associated PC of the reanalysis result, several models (i.e. cnrm_cm3, ncar_pcm1, ipsl_cm4, and ukmo_hadcm3) reproduce an opposite variability pattern in spatial distribution, indicating the failure simulation on interannual variability (Zhou and Yu, 2006; Zhang *et al*., 2008).

To check whether the first leading mode of zonal wind at 200 hPa represents the meridional displacement of the AJS, we perform a composite analysis. The composites are calculated when the absolute values of the normalized PC of EOF-1 modes are larger than 0.5. Compared to the observed AJS shifting meridionally between 39°N and 43°N (Figure 5(w)), 10 out of 22 models (bccr_bcm2_0, cccma_cgcm3_1_t63, cnrm_cm3, gfdl_cm_2_0, gfdl_cm2_1, ipsl_cm4, miroc3_2_hires, mpi_echam5, ncar_ccsm3_0, and ukmo_hadgem1) could simulate successfully the south–north displacement, but the simulated AJS locations in some models such as cnrm_cm3 and ukmo_hadgem1 (ipsl_cm4) tend to move more poleward (equatorward). In these 10 models, 2 models (gfdl_cm_2_0 and gfdl_cm2_1) could reproduce the observed SAT cooling changes in mid-eastern China in the late 20th century (Figure 1). The first leading modes of the other 12 models simulations (i.e. bcc_cm1, cccma_cgcm3_1, csiro_mk3_0, giss_aom, giss_model_e_h, giss_model_e_r, iap_fgoals1_0_g, inmcm3_0, miroc3_2_medres, mri_cgcm2_3_2a, ncar_pcm1, and ukmo_hadcm3) could not capture the feature of AJS meridional displacement, but the intensity changes of AJS, especially in cccma_cgcm3_1, inmcm3_0, mri_cgcm2_3_2a and ncar_pcm1. That is to say, more than half the models (12 out of 22) could not reproduce the distinct feature of AJS meridional displacement. Previous studies (Liang *et al*., 2001; Lu, 2004; Zhang and Guo, 2005) suggested that the changes in the AJS, in particular its variation of meridional location, can greatly influence the East Asian summer climate. It is found that the performances of the AJS meridional shifting changes in most IPCC AR4 models are poor. Therefore, the failure of the SAT simulation in mid-eastern China may be contributed to the AJS biases (Figure 2). We point out that although the performances of miroc3_2_medres in simulating the displacements of the AJS are poor (Figsures 2(a), 3(p), 4(p) and 5(p)), it still simulates the SAT cooling in mid-eastern China during the late 20th century (Figure 1), indicating that other factors could also influence the SAT biases besides the AJS meridional displacement.

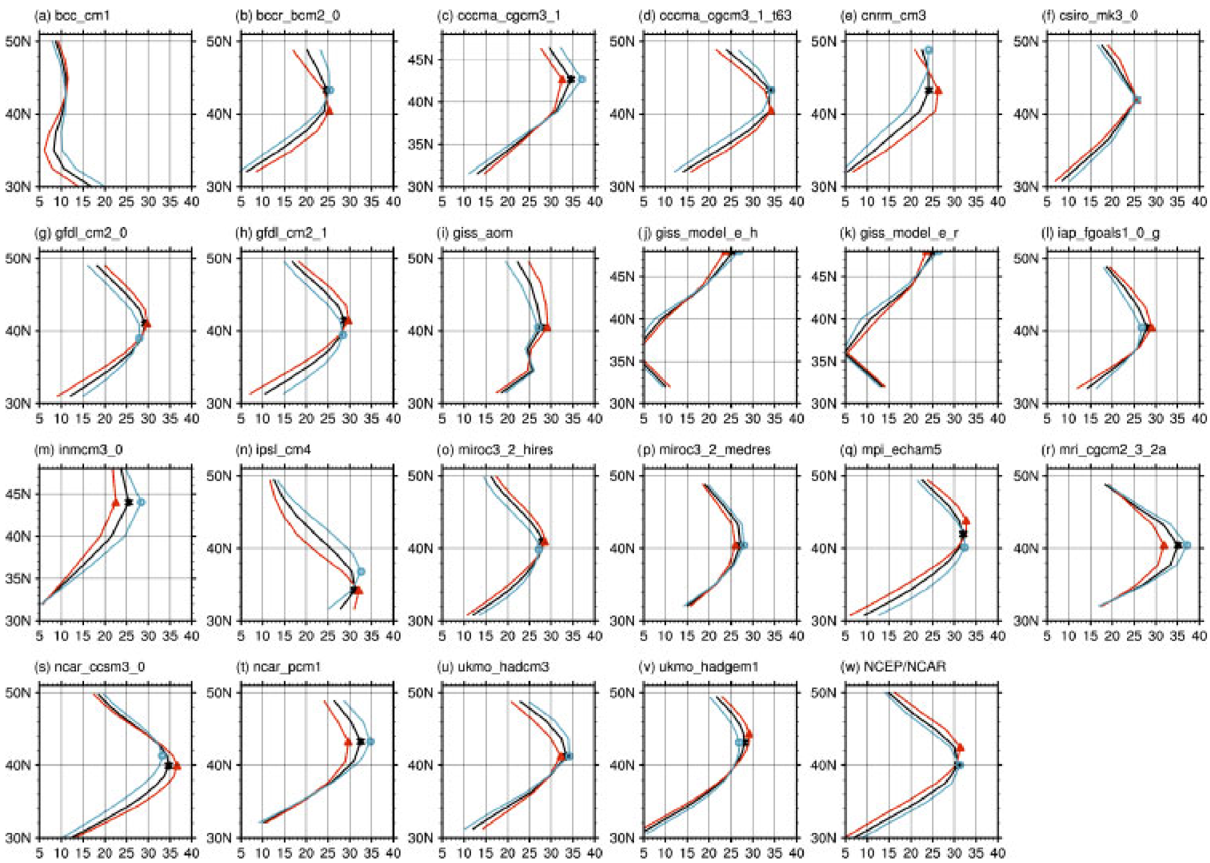

Figure 5. The red (blue) lines are the composite of 200 hPa zonal wind averaged between 75° and 105 °E in terms of PC-1 values greater (less) than 0.5 (−0.5) variance. The black lines are the corresponding climatology of 200 hPa zonal wind. The marked dot indicates the maximum of averaged zonal wind. This figure is available in colour online at wileyonlinelibrary.com/journal/joc

5. Linkage between the AJS and SAT in models

Observational results have shown that the summer SAT anomalies in mid-eastern China are closely related to the variations of AJS location (Liang *et al*., 2001; Zhang and Guo, 2005; Yu and Zhou, 2007). Accompanying the poleward displacement of the AJS, Figure 7(k) shows significant sinking motions over north to 25°N, indicating a SAT warming. A multi-decadal variation of the AJS with equatorward displacement is observed in the late 1970s (Figures 8(k) and 9(k)), which is thus responsible for the SAT cooling change in mid-eastern China during the second half of the 20th century. In Section 4, it has been shown that 10 models could well perform the meridional variations of the AJS. A question thus arises as to why only two of them could simulate successfully the surface cooling in mid-eastern China in the second half of the 20th century. To answer this question, we would like to examine the AJS meridional displacements and their relationships with the SAT in mid-eastern China in these ten models. The ten models are catalogued into three groups. The first group includes the models that did a good job in simulating the mid-eastern China SAT (upper row in Figures 7, 8 and 9). The other eight SAT poor-performance models are sub-classified into the second and third groups in terms of relationships between the AJS meridional displacement and the mid-eastern China SAT (the second and third rows in Figures 7, 8 and 9). For the sake of convenience, the corresponding PC of the first leading EOF mode in several models (bccr_bcm2_0, cccma_cgcm3_1_t63, cnrm_cm3, ipsl_cm4, and ncar_ccsm3_0) is multiplied by−1.0 to make sure that the negative (positive) values of PC represent the AJS equatorward (poleward) shift (Figure 8). In order to detect the approximate time points of the significant trend change, the sequential Mann-Kendall (SMK) test (Gerstengarbe and Werner, 1999) is applied on the first leading PC in the 10 models and the NCAR/NCEP reanalysis series (Figure 9). SMK test is a nonparametric test, and usually used to detect the time points of trend changes in time series. Additional details about the SMK test can be found in Gerstengarbe and Werner (1999) and Li *et al*. (2011). The results of the 11-year running means and SMK test for the first leading PC in the observation reveal that there is an abrupt change in the summer AJS equatorward shift in the late 1970s (Figures 8(k) and 9(k)).

5.1. The first group

Two models of gfdl_cm2_0 and gfdl_cm2_1 reproduce the SAT cooling in mid-eastern China (Figure 1). In these two models, the AJS shows apparent multi-decadal meridional displacement variations, and the AJS tends to shift euqatorward during the mid-1980s (Figures 8(a), and (b), 9(a) and (b)). The significantly positive relationship between the AJS meridional displacement and SAT in mid-eastern China in gfdl_cm2_1 (Figure 6) is consistent with the observed result (Liang *et al*., 2001; Zhang and Guo, 2005). However, the negative relationship in

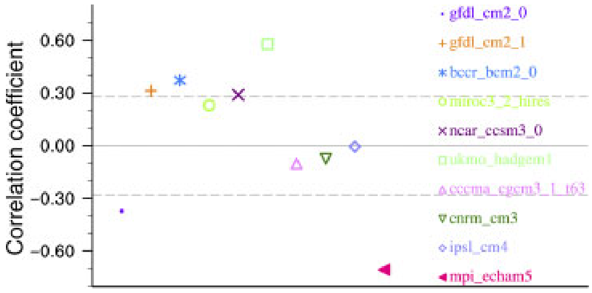

Figure 6. Correlation coefficients between PC-1 and mid-eastern China SAT (25°–35°N, 105°–120 °E) in the ten models. The dashed lines indicate 95% significance level. The PCs in bccr_bcm2_0, cccma_cgcm3_1_t63, cnrm_cm3, ipsl_cm4, and ncar_ccsm3_0 are multiplied by−1.0, indicating that the negative values mean southward displacements of the AJS. This figure is available in colour online at wileyonlinelibrary.com/journal/joc

gfdl_cm_2_0 is opposite to the observation (Figure 6). On the basis of the meridional circulation changes, it could be inferred that the AJS equatorward shifts in gfdl_cm2_1 are accompanied with the SAT cooling in mid-eastern China because of ascending motions over north to 25°N (Figure 7(b)) which result from the anomalous divergence at the high-level troposphere and convergence at the low-level troposphere over eastern Asia (not shown). The dynamical connection between the AJS and SAT in mid-eastern China in gfdl_cm2_0 (Figure 7(a)) contradicts the linear relationships in Figure 6. This indicates that other simulated climate signals impact the mid-eastern SAT more than the AJS does in the model of gfdl_cm2_0.

5.2. The second group

In this group, the models could reproduce the positive relationship between the mid-eastern China SAT and the AJS meridional displacement (Figure 6). In miroc3_2_hires and ncar_ccsm3_0, the equatorward displacement of the AJS is associated with anomalous divergence at the upper-level troposphere and convergence at the lower-level troposphere over eastern China (not shown) which result in the anomalous air ascent motions (Figure 7(d) and (e)). Thus, the SAT tends to be cooling, agreeing with the positive linear relationship between the mid-eastern China SAT and the AJS meridional displacement. However, in the miroc3_2_hires simulation, the multi-decadal change of the AJS meridional displacement in the late 1980s (Figures 8(d) and 9(d)) is delayed in comparison with observation (Figures 8(k) and 9(k)), inducing from the SAT biases in Figure 1. It is noted that the mid-eastern China SAT during 1987–1999 is about 0.11 °C cooler than that during 1961–1986 in miroc3_2_hires, which is in accordance with the AJS multi-decadal changes and their impacts on the mid-eastern China SAT. Bccr_bcm2_0 and ncar_ccsm3_0 fails to simulate the AJS equatorward shift in the 1980s (Figures 8(c) and, (e), and 9(c) and (e)), which causes the warm SAT biases in mid-eastern China (Figure 1). These results show that the mid-eastern China SAT biases

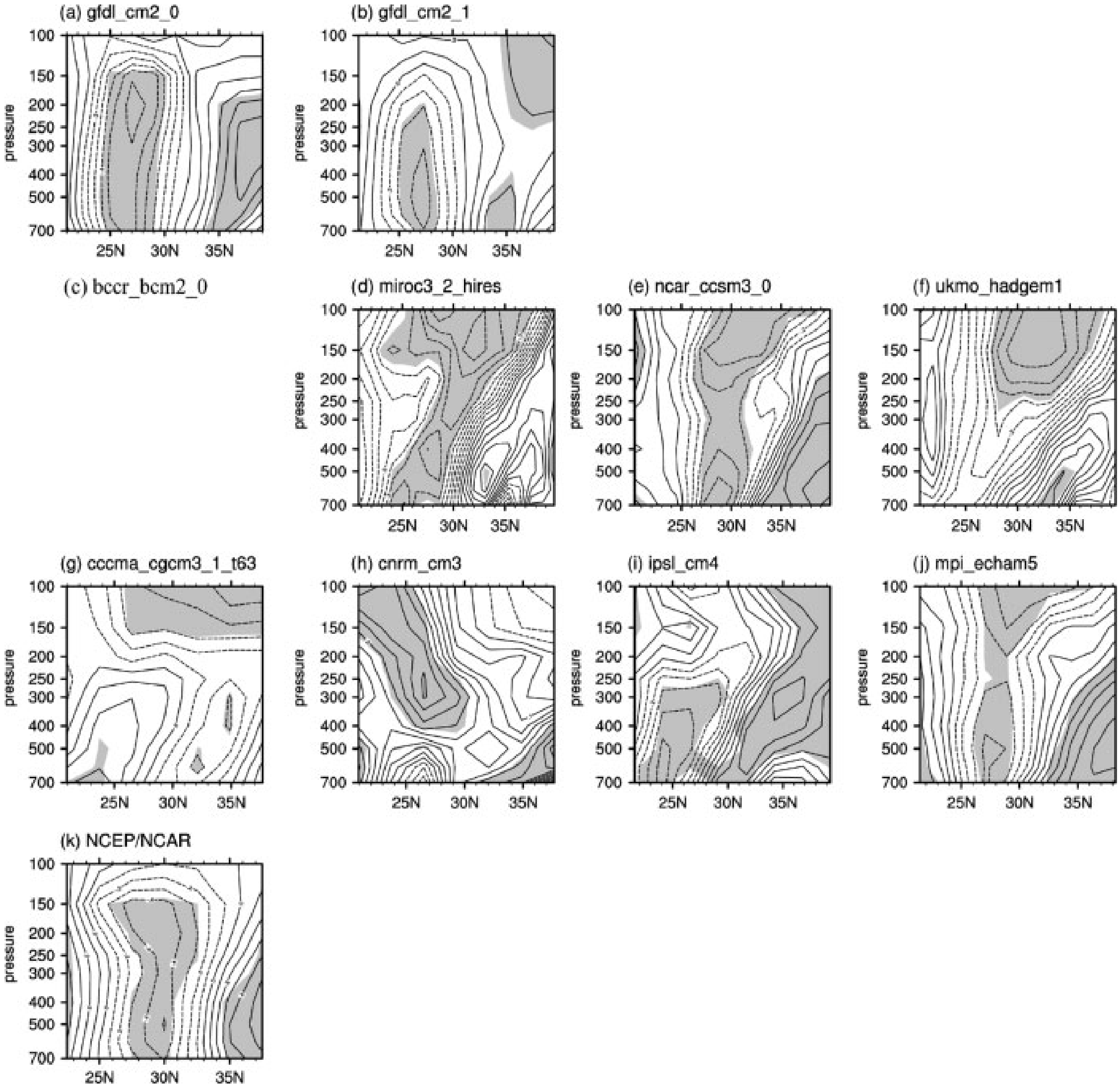

Figure 7. Regression coefficient patterns of averaged vertical velocity (between 105° and 120 °E) against PC-1 in models and the NCAR/NCEP reanalysis. The negative value represents sinking motion. The shadings are exceeding 90% significant level. The vertical velocity of bccr_bcm2_0 is not available. The PCs in cccma_cgcm3_1_t63, cnrm_cm3, ipsl_cm4, and ncar_ccsm3_0 are multiplied−1.0, indicating that the negative values mean southward displacements of the AJS.

could be contributed by the poor performances of the AJS meridional displacement on multi-decadal timescales in bccr_bcm2_0, miroc3_2_hires and ncar_ccsm3_0.

Although the correlation between the AJS and the SAT in ukmo_hadgem1 is the largest (Figure 6), their dynamical linkage through large-scale atmospheric circulation anomalies is poorly simulated as shown in Figure 7(f). The underestimated impact of the AJS meridional displacement on large-scale circulations indicates the role of the AJS in mid-eastern China SAT bias.

5.3. The third group

In comparison, the correlations between the mid-eastern China SAT and AJS meridional displacement in this group are weakly negative (cccma_cgcm33_1_t63, cnrm_cm3, and ipsl_cm4) or significantly negative (mpi_echam5) as shown in Figure 6. The meridional circulation anomalies associated with the AJS meridional displacement do not exceed 90% significant level in cccma_cgcm33_1_t63, cnrm_cm3 and ipsl_cm4 (Figure 7(g–i)). These underestimated circulation anomalies related to the south–north displacement of the AJS could result in the SAT biases in mid-eastern China. Cccma_cgcm3_1_t63 and mpi_echam5 fail to reproduce the regime shift of AJS equatorward shift (Figs. 8g, 8j, 9g, and 9j). In mpi_echam5, the equatorward displacement of the AJS in the late 1980s (Figures 8(j) and 9(j)) is associated with significant ascent motion over the mid-eastern China (Figure 7(j)), and thus, the mid-eastern SAT is expected to be cool. However, the simulation of SAT change and its relationship with the AJS in mpi_echam5 is different from the expectation (Figure. 1), indicating that other factors exert an influence on the SAT biases.

Though all ten models could reproduce the changes of the AJS south–north displacement, the performances of models in simulating the multi-decadal variations of the AJS meridional displacement and their induced atmospheric circulation anomalies over eastern China

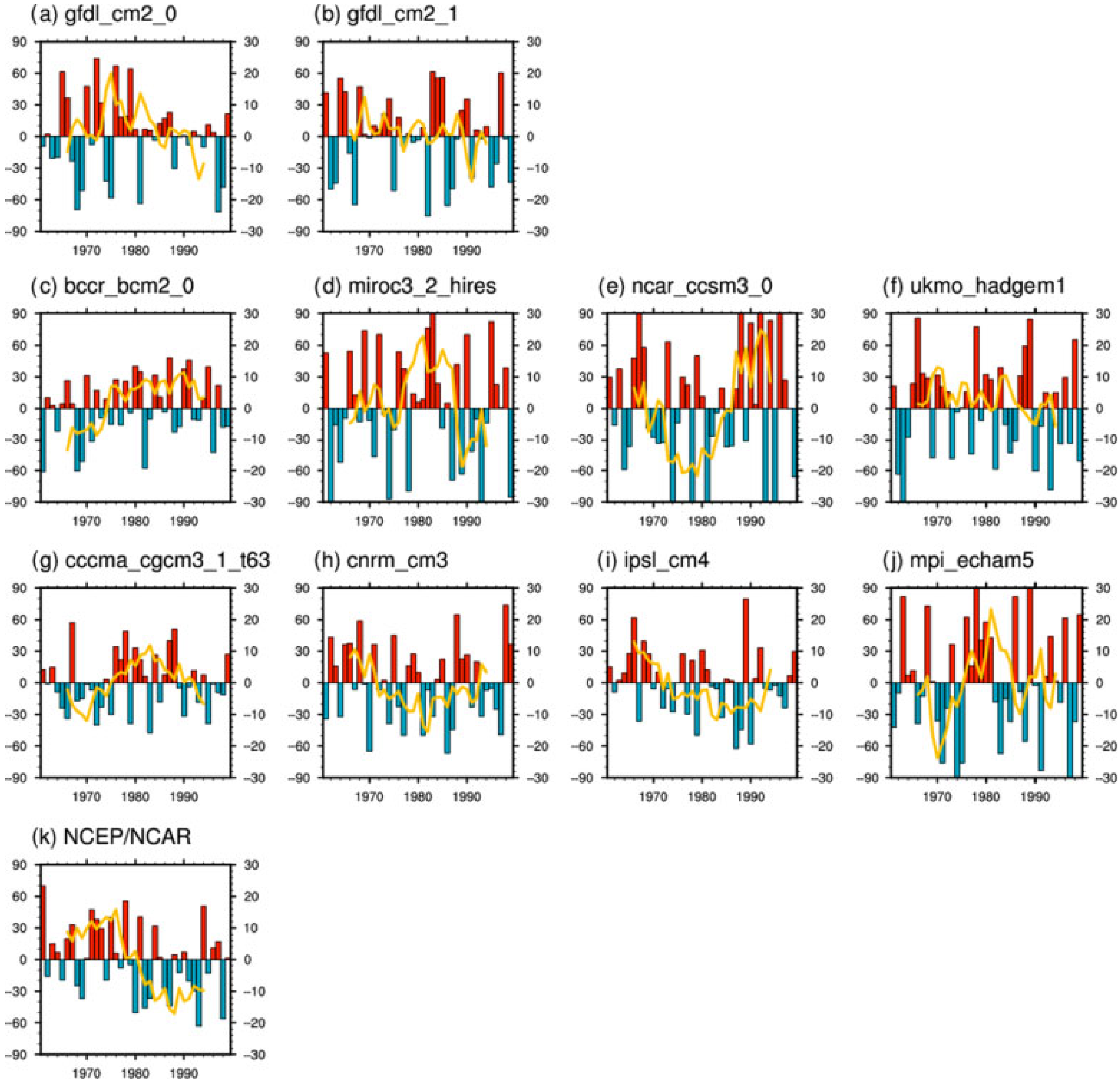

Figure 8. The first leading PC in the 10 models and the NCAR/NCEP reanalysis. The yellow lines are 11-year running mean. The PCs in bccr_bcm2_0, cccma_cgcm3_1_t63, cnrm_cm3, ipsl_cm4, and ncar_ccsm3_0 are multiplied by−1.0, indicating that the negative values mean southward displacements of the AJS. This figure is available in colour online at wileyonlinelibrary.com/journal/joc

are the key factors. Because the multi-decadal variations of the AJS simulated in bccr_bcm2_0, ncar_ccsm3_0 and cccma_cgcm3_1_t63 are opposite to the observation, their SAT performances in mid-eastern China are opposite to the observed. Most of the ten models, such as cccma_cgcm3_1_t63, cnrm_cm3 and ipsl_cm4, and ukmo_hadgem1, underestimate the influences of the AJS meridional displacement on meridional circulations over eastern China. This, thus, causes the simulated SAT biases in mid-eastern China.

6. Discussion and summary

6.1. Discussion

The performance of the AJS meridional displacement on multi-decadal timescales and its associated atmospheric circulation anomalies are very important for successfully simulating the SAT changes in mid-eastern China. However, even though there is no evident south–north displacement of the AJS in the simulations of miroc3_2_medres (Fig. 5p), the SAT cooling in mid-eastern China is still reproduced in the late 1970s (Figure 1). In gfdl_cm2_0 and mpi_echam5, although the multi-decadal variations of the AJS meridional displacement (Figure 5(g) and (q)) and their associated large-scale circulation anomalies over eastern China (Figure 7(a) and (j)) are both significant, the relationships between the AJS and SAT in mid-eastern China are significantly opposite to the observation (Figure 6). These results indicate that the biases of the SAT in mid-eastern China may also be contributed to other possible systematical factors instead of the AJS. Zhou *et al*. (2009) have reviewed possible

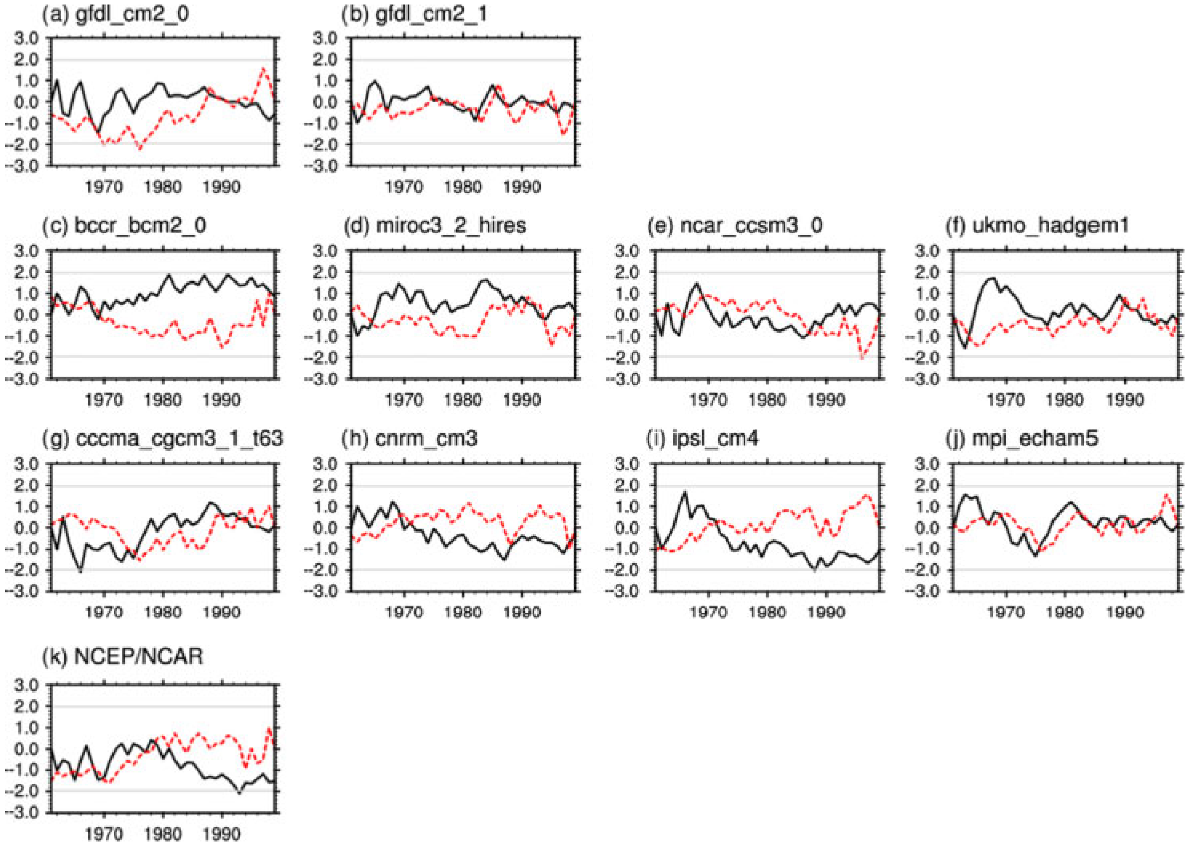

Figure 9. The progressive (solid) or retrograde (dashed) scores of the first leading PC in the 10 models and the NCAR/NCEP reanalysis calculated by the SMK test, where the confidence limits (±1.96) are shown as horizontal gray lines. The crossing point of progressive and retrograde scores indicates that a multi-decadal change occurred at that time. This figure is available in colour online at wileyonlinelibrary.com/journal/joc

causes of the multi-decadal variability of the EASM, including the influences of the tropical ocean warming, the heat flux forcing of the Tibetan Plateau, the aerosol forcing, and internal variability. Except the influences of anthropogenic aerosols forcing, these possible factors in models are likely systematically associated with the SAT biases in mid-eastern China. Owing to underestimating the influences of the AJS on meridional circulations over eastern China, cccma_cgcm3_1_t63, cnrm_cm3, ipsl_cm4, and ukmo_hadgem1 perform poorly in the simulation of SAT in mid-eastern China. Nonetheless, it is still possible that the SAT biases in mid-eastern China may result from other factors besides the AJS.

Previous studies have shown the important effects of tropical sea surface temperature anomalies (SSTa) on EASM (i. e. Chang *et al*., 2000; Lau and Wu, 2001; Wang *et al*., 2006; Nagataa and Mikamib, 2010). Zhou and Yu (2006) suggested that a great part of the observed surface atmospheric temperature variation over China can be reproduced by SST forcing. The poor performances of summer rainfall in the Asian–Australian monsoon region are due to the lack of skill in the relationship between rainfall and SST anomalies over the Philippine Sea (Wang *et al*., 2004). Many efforts have been made to evaluate tropical Pacific SST simulation in IPCC AR4 (e.g. van Oldenborgh *et al*., 2005; Capotondi *et al*., 2006; Wang *et al*., 2009). Therefore, the tropical SST biases may be the other important factor being responsible for the summer monsoon biases in East Asia. Figure 10 identifies that the significant SST biases related to the SAT biases in mid-eastern China are in the western tropical Pacific. This indicaties that the improvement of the SAT simulation in mid-eastern China also depends on the reliability of the western tropical Pacific SST. The SST biases over the western tropical Pacific may lead to biases of the ITCZ convective heating, which then produce the biases of meridional teleconnections or meridional circulations, and therefore, lead to poor simulations over eastern China (Liang and Wang, 2001).

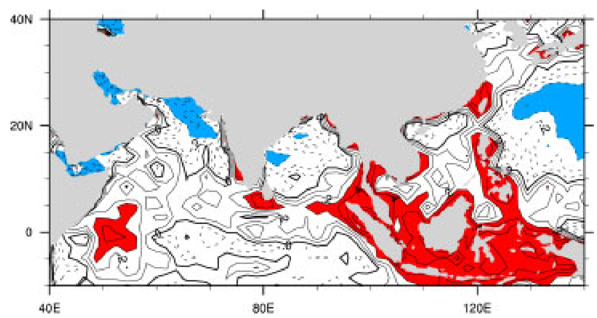

Figure 10. Uncentred point-wise correlation pattern between the summer SST biases and surface temperature biases averaged in the region of 25°–35°N, 105°–120°E. The shading is exceeding 90% significant level. This figure is available in colour online at wileyonlinelibrary.com/journal/joc

6.2. Summary

Three out of 22 IPCC AR4 models can simulate the observed SAT cooling in mid-eastern China in the late 1970s. This summer SAT biases may arise from many factors (Zhou *et al*., 2009). According to the bias analysis in IPCC AR4 models, it is found that the summer SAT biases in mid-eastern China are related to the upper-level extratropical zonal wind located north of the observed summer climatology AJS core. To illustrate how the AJS biases impact the summer SAT performances in mid-eastern China, the simulations of the AJS in IPCC AR4 models are assessed. Climatologically, the cores of the summer AJS in more than half the models are north of those observed, and most of the models underestimate the intensity of the summer AJS.

The observed results have revealed that the summer AJS change features its south–north displacement, which has a strong linkage with surface climate anomalies in eastern China (Lau *et al*., 2000; Liao *et al*., 2004; Yu and Zhou, 2007). On the basis of the results of EOF analysis, our studies found that only 10 models (bccr_bcm2_0, cccma_cgcm3_1_t63, cnrm_cm3, gfdl_cm_2_0, gfdl_cm2_1, ipsl_cm4, miroc3_2_hires, mpi_echam5, ncar_ccsm3_0, and ukmo_hadgem1) have the ability to capture the equatorward shift of the AJS meridional displacement. It is noted that there are merely 2 of these 10 models successfully simulating the SAT cooling in mid-eastern China in the late 1970s. To investigate the mid-eastern summer SAT biases, we further examine the simulations of the summer AJS meridional displacement and the associated anomalous large-scale circulations. Owing to the good performance of the AJS meridional displacement and associated circulation anomalies, gfdl_cm_2_1 could simulate successfully the SAT cooling in mid-eastern China in the second half of the 20th century. The AJS meridional displacement in miroc3_2_hires is in the late 1980s, being later than the observation, whereas, it tends to shift northward in ncar_ccsm3_0. The failure in temporal variation of the AJS leads to the SAT warming biases in miroc3_2_hires and ncar_ccsm3_0. Although the AJS variations on multi-decadal timescales are similar to the observed, the influences of the AJS on large-scale circulations over eastern China are underestimated in cnrm_cm3 and ipsl_cm4, cccma_cgcm3_1_t63, and ukmo_hadgem1, causing the SAT biases in mid-eastern China.

In summary, this study identifies that the performances on the AJS meridional displacement and the associated anomalous large-scale circulations are greatly responsible for the summer SAT changes over mid-eastern China. To improve the model reliability on simulating the EASM, the perspectives of dynamic configuration at mid-latitude of the troposphere needs to be studied further.

Acknowledgements

This research was sponsored by the National Basic Research Program of China (973 Program, No. 2011CB 403504), Natural Science Foundation of China (Grants Nos. U0733002, 40906010 and 2009CB4214401), and City University of Hong Kong (Strategic Research Grant No. 7002717).

References

Capotondi A, Wittenberg A, Masina S. 2006. Spatial and temporal structure of tropical Pacific interannual variability in 20th century coupled simulations. *Ocean Model* **15**: 274–298.

Chang C-P, Zhang Y, Li T. 2000. Interannual and Interdecadal Variations of the East Asian Summer Monsoon and Tropical Pacific SSTs. Part I: Roles of the Subtropical Ridge. *Journal of Climate* **13**: 4310–4325.

Ding Y, Sun Y. 2003. Long-term climate variability in China. WMO/TD No. 1172, 18–33.

Ding Y, Sun Y, Wang Z, Zhu Y, Song Y. 2009. Inter-decadal variation of the summer precipitation in China and its association with decreasing Asian summer monsoon Part II: Possible causes. *International Journal of Climatology* **29**: 1926–1944.

Ding Y, Wang Z, Sun Y. 2008. Inter-decadal variation of the summer precipitation in East China and its association with decreasing Asian summer monsoon. Part I: Observed evidences. *International Journal of Climatology* **228**: 1139–1161.

Folland CK, Karl TR, Christy JR, Clarke RA, Gruza GV, Jouzel J, Mann ME, Oerlemans J, Salinger MJ, Wang S-W. 2001a. Observed climate variability and change. In *Climate change 2001. The Scientific Basis*, Houghton JT, Ding Y, Griggs DJ, Noguer M, van der Linden PJ, Dai X, Maskell K, Johnson CA (eds). Cambridge University Press: Cambridge, United Kingdom and New York, NY, 99–181.

Folland CK, Rayner NA, Brown SJ, Smith TM, Shen SSP, Parker DE, Macadam I, Jones PD, Jones RN, Nicholls N, Sexton DMH. 2001b. Global temperature change and its uncertainties since 1861. *Geophysical Research Letters* **28**: 2621–2624, DOI: 10.1029/2001GL012877.

Gerstengarbe FW, Werner PC. 1999. Estimation of the beginning and end of recurrent events within a climate regime. *Climate Research* **11**: 97–107.

Gong D-Y, Ho C-H. 2003. Arctic Oscillation signals in the East Asian summer monsoon. *Journal of Geophysical Research* **108**: 4066, DOI: 10.1029/2002JD002193.

Hu Z, Yang S, Wu R. 2003. Long-term climate variations in China and global warming signals. *Journal of Geophysical Research* **108**: 4614, DOI: 10.1029/2003JD003651.

Jones PD, New M, Parker DE, Martin S, Rigor IG. 1999. Surface air temperature and its changes over the past 150 years. *Reviews of Geophysics* **37**: 173–199, DOI: 10.1029/1999RG900002.

Kistler R, Kalnay E, Collins W, Saha S, White G, Woollen J, Chelliah M, Ebisuzaki W, Kanamitsu M, Kousky V, van den Dool H, Jenne R, Fiorino M. 2001. The NCEP-NCAR 50-Year Reanalysis: Monthly Means CDROM and Documentation. *Bulletin of the American Meteorological Society* **82**: 247–268.

Lau K-M, Kim K-M, Yang S. 2000. Dynamical and Boundary Forcing Characteristics of Regional Components of the Asian Summer Monsoon. *Journal of Climate* **13**: 2461–2482.

Lau K-M, Wu HT. 2001. Principal Modes of Rainfall-SST Variability of the Asian Summer Monsoon: A Reassessment of the Monsoon-ENSO Relationship. *Journal of Climate* **14**: 2880–2895.

Li Y, Lu H, Jarvis MJ, Clilverd MA, Bates B. 2011. Nonlinear and nonstationary influences of geomagnetic activity on the winter North Atlantic Oscillation. *Journal of Geophysical Research* **116**: D16109, DOI: 10.1029/2011JD015822.

Li L, Wang B, Zhou T. 2007. Contributions of natural and anthropogenic forcings to the summer cooling over eastern China: An AGCM study. *Geophysical Research Letters* **34**: L18807, DOI: 10.1029/2007GL030541.

Liang X-Z, Wang W-C. 1998. Associations between China monsoon rainfall and tropospheric jets. *Quarterly Journal of the Royal Meteorological Society* **124**: 2597–2623.

Liang X-Z, Wang W-C, Samel AN. 2001. Biases in AMIP model simulations of the east China monsoon system. *Climate Dynamics* **17**: 291–304.

Liao Q, Gao S, Wang H, Tao S. 2004. Anomalies of the extratropical westerly Jet in the north hemisphere and their impacts on east Asian summer monsoon climate anomalies (in Chinese). *Chinese Journal of Geophysics* **47**: 10–18.

Lin Z, Lu R. 2005. Interannual Meridional Displacement of the East Asian Upper-tropospheric Jet Stream in Summer. *Advances in Atmospheric Sciences* **22**: 199–211.

Lu R. 2004. Associations among the components of the East Asian summer monsoon systems in the meridional direction. *Journal of the Meteorological Society of Japan* **82**: 155–165.

Menon S, Hansen J, Najarenko L, Luo Y. 2002. Climate effects of black carbon aerosols in China and India. *Science* **297**: 2250–2252.

Nagataa R, Mikamib T. 2010. Response of the summer atmospheric circulation over East Asia to SST variability in the tropical Pacific. *International Journal of Climatology* **30**: 813–826, DOI: 10.1002/joc.1909.

Nitta T, Hu ZZ. 1996. Summer climate variability in China and its association with 500hPa height and tropical convection. *Journal of the Meteorological Society of Japan* **74**: 425–445.

Qian Y, Giorgi F. 1999. Interactive coupling of regional climate and sulfate aerosol models over eastern Asia. *Journal of Geophysical Research* **104**: 6477–6499.

Qian Y, Leung LR, Ghan SJ, Giorgi F. 2003. Effects of increasing aerosol on regional climate change in China: Observation and modeling. *Tellus* **55B**: 914–934.

Raisanen J. 2007. How reliable are climate models? *Tellus* **59A**: 2–29.

Sun Y, Ding Y. 2008. An assessment on the performance of IPCC AR4 climate models in simulating interdecadal variations of the East Asian Summer Monsoon. *Acta Meteorologica Sinica* **22**: 472–488.

Ueda H, Iwai A, Kuwako K, Hori ME. 2006. Impact of anthropogenic forcing on the Asian summer monsoon as simulated by eight GCMs. *Geophysical Research Letters* **33**: L06703, DOI: 10.1029/2005GL025336.

van Oldenborgh GJ, Philip SY, Collins M. 2005. El Niño in a changing climate: A multi-model study. *Ocean Science* **1**: 81–95.

Wang B, Kang IS, Lee JY. 2004. Ensemble Simulations of Asian–Australian Monsoon Variability by 11 AGCMs. *Journal of Climate* **17**: 803–818.

Wang X, Li C, Zhou W. 2006. Interdecadal variation of the relationship between Indian rainfall and SSTA modes in the Indian Ocean. *International Journal of Climatology* **26**: 595–606.

Wang X, Wang D, Zhou W. 2009. Decadal variability of twentieth century El Niño and La Niña occurrence from observations and IPCC AR4 coupled models. *Geophysical Research Letters* **36**: L11701, DOI: 10.1029/2009GL037929.

Wang X, Wang C, Zhou W, Wang D, Song J. 2011. Teleconnected influence of North Atlantic sea surface temperature on the El Niño onset. *Climate Dynamics* **37**: 663–676, DOI: 10.1007/s00382-010-0833-z.

Xu Q. 2001. Abrupt change of the mid-summer climate in central east China by the influence of atmospheric pollution. *Atmospheric Environment* **35**: 5029–5040.

Yu R, Wang B, Zhou T. 2004. Tropospheric cooling and summer monsoon weakening trend over East Asia. *Geophysical Research Letters* **31**: L22212, DOI: 10.1029/2004GL021270.

Yu R, Li J, Yuan W, Chen H. 2010. Changes in characteristics of late-summer precipitation over eastern China in the past 40 years revealed by hourly precipitation data. *Journal of Climate* **23**: 3390–3396.

Yu R, Zhou T. 2007. Seasonality and three-dimensional structure of the interdecadal change in East Asian monsoon. *Journal of Climate* **20**: 5344–5355.

Zhang Y, Guo L. 2005. Relationship between the simulated East Asian westerly jet biases and seasonal evolution of rainbelt over eastern China. *Chinese Science Bulletin* **50**: 1503–1508.

Zhang Y, Takahashi M, Guo L. 2008. Analysis of the East Asian subtropical westerly jet simulated by CCSR/NIES/FRCGC coupled climate system model. *Journal of the Meteorological Society of Japan* **86**: 257–278.

Zhou T, Gong D, Li J, Li B. 2009. Detecting and understanding the multi-decadal variability of the East Asian Summer Monsoon – Recent progress and state of affairs. *Meteorology* **Z18**: 455–467.

Zhou T, Yu R. 2006. Twentieth-Century Surface Air Temperature over China and the Globe Simulated by Coupled Climate Models. *Journal of Climate* **19**: 5843–5858.

Zhou W, Li C, Chan JCL. 2006. The interdecadal variations of the summer monsoon rainfall over South China. *Meteorology and Atmospheric Physics* **93**: 165–175, DOI: 10.1007/S00703-006-018-9.

